J|A|C|S ARTICLES

Published on Web 10/08/2010

Ferromagnetically Coupled Cobalt−Benzene−Cobalt: The Smallest Molecular Spin Filter with Unprecedented Spin Injection Coefficient

Sabyasachi Sen[†] and Swapan Chakrabarti*[,‡]

Department of Physics, JIS College of Engineering, Block-A, Phase-III, Kalyani, Nadia PIN-741235, India, and Department of Chemistry, University of Calcutta, 92, APC Road, Kolkata 700 009, India

Received July 28, 2010; E-mail: swapanchem@yahoo.co.in

Abstract: Here, we predict that the ferromagnetically coupled cobalt−benzene−cobalt system will act as the smallest molecular spin filter with unprecedented spin injection coefficient. To validate our in-silico observation, we have performed state-of-the-art nonequilibrium Green's function calculations and analyzed the density of states of cobalt at the relativistic and nonrelativistic level of theory. Remarkably, we found that unpaired 3d electrons of cobalt are not participating in the spin transport process like other transition metal containing multidecker complexes. Instead, an admixture of the outer-sphere 4s and 4p orbitals of cobalt along with the 2p orbital of carbon of the benzene moiety is contributing to the singly occupied highest molecular orbital in the majority spin channel that creates a path for coherent spin transport leading to the extremely high spin injection coefficient of the system. The absence of the 3d electrons of cobalt in the spin transport process has been carefully examined, and it was found that the nodal structure of the 3d orbital of cobalt is not at all suitable for bonding in the cobalt−benzene−cobalt system. The whole study indicates that the underlying mechanism of the spin filter action in cobalt−benzene−cobalt is completely distinctive from the other known materials.

1. Introduction

The subject of spintronics utilizes quantum transport of electron spin as an information carrier in addition to its charge degree of freedom.[1−4] At the molecular level, spintronics is still in its rudimentary stage; however, there is ample theoretical and experimental evidence,[1−4] which establishes the significance of the field in the perspective of nanodevice fabrication. In spintronic materials, the spin orientations of the conduction electrons survive for a relatively longer time, which makes them a potential candidate to be useful in a wide variety of applications starting from memory storage, high speed quantum computing devices, to magnetic sensors.[5,6] Of the many promising areas of molecular spintronics, spin filter material is the one where electronic current is spin-polarized with the coexistence of metallic feature in one spin channel and insulating in the other. The degree of spin filter action is expressed in terms of an efficiency parameter and can be calculated by evaluating the current at different bias voltage in the two spin states. Earlier, Son and co-workers[7] reported the direct interplay of external electric field and electron spin degree of freedom in graphene nanoribbons. Min and co-workers demonstrated spin filter action in Au−V(Cr) quantum wires adsorbed on an armchair (5, 5) boron nitride nanotube.[8] The spin filter action has also been predicted in sandwiched molecular systems like a one-dimensional (1D) organometallic chain comprised of vanadium−iron−cyclopentadienyl, $[VCpFeCp]_n$, systems and $(CpFeCpV)_n$ multidecker wire.[9,10] Herrmann and his group reported that organic radicals can also act as potential molecular spin filter.[11] All of these molecular systems are relatively complex, and moreover the spin filter efficiency was calculated only at zero bias, leaving a question mark on the reliability of the results in the presence of the applied electric field. With an ever increasing aspiration to explore "plenty of room at the bottom", here we demonstrate theoretically that a much smaller and uncomplicated molecular system can display a giant bias-dependent spin filter action that has never been envisaged before. We have considered the cobalt−benzene−cobalt (CBC) system adsorbed on the Au (111) surface as our model system, and it is shown in Figure 1. On this molecular setup, we have performed spin-polarized quantum transport calculation with an aim to evaluate the zero

[†] JIS College of Engineering.
[‡] University of Calcutta.

(1) Xiong, Z. H.; Wu, D.; Valy Vardeny, Z.; Shi, J. *Nature* **2004**, *427*, 821.
(2) Kikkawa, J. M.; Awschalom, D. D. *Nature* **1999**, *397*, 139.
(3) Son, Y. W.; Cohen, M. L.; Louie, S. G. *Nano Lett.* **2007**, *7*, 3518.
(4) Min, Y.; Yao, K. L.; Liu, Z. L.; Cheng, H. G.; Zhu, S. C.; Gao, G. Y. *J. Magn. Magn. Mater.* **2009**, *321*, 312.
(5) Pati, R.; Senapati, L.; Ajayan, P. M.; Nayak, S. K. *Phys. Rev. B* **2003**, *68*, 100407(R).
(6) Friend, R. H.; Gymer, R. W.; Holmes, A. B.; Burroughes, J. H.; Marks, R. N.; Taliani, C.; Bradley, D. D. C.; Dos Santos, D. A.; Brédas, J. L.; Lögdlund, M.; Salaneck, W. R. *Nature* **1999**, *397*, 121.
(7) Son, Y.-W.; Cohen, M. L.; Louie, S. G. *Nature* **2006**, *444*, 347.
(8) Min, Y.; Yao, K. L.; Liu, Z. L.; Gao, G. Y.; Cheng, H. G.; Zhu, S. C. *Nanotechnology* **2009**, *20*, 095201.
(9) Zhou, L. P.; Yang, S.-W.; Ng, M.-F.; Sullivan, M. B.; Tan, V. B. C.; Shen, L. *J. Am. Chem. Soc.* **2008**, *130*, 4023.
(10) Wu, J.-C.; Wang, X.-F.; Zhou, L.; Da, H.-X.; Lim, K. H.; Yang, S.-W.; Li, Z.-Ya. *J. Phys. Chem. C* **2009**, *113*, 7913.
(11) Herrmann, C.; Solomon, G. C.; Ratner, M. A. *J. Am. Chem. Soc.* **2010**, *132*, 3682.

10.1021/ja106705m © **2010 American Chemical Society**

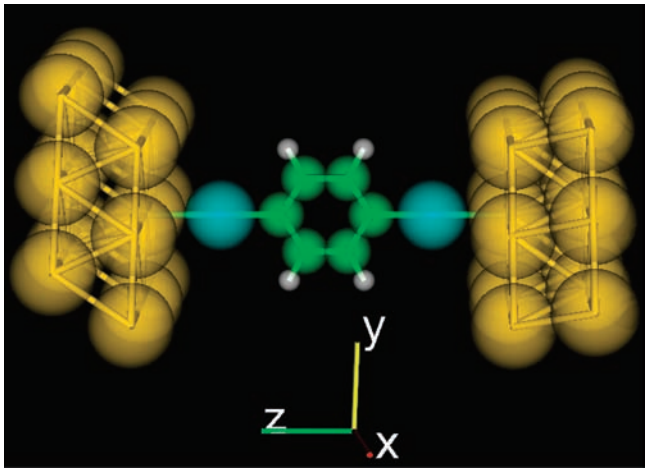

Figure 1. Schematic representation of Co−benzene−Co adsorbed on Au (111) surface.

bias equilibrium spin filter efficiency (ESFE) and bias-dependent spin injection coefficients (BDSIC) as well. Both ESFE and BDSIC of the proposed device are found to be extremely large, and to the best of our knowledge the values of BDSIC for our system are unprecedented.

2. Computational Details

In the present work, the geometry of the CBC attached with a layer of Au electrode has been optimized with all possible spin states under the influence of static electric field up to 1 V. We found that the septet state is the most stable state and the structure of CBC is symmetric up to 0.8 V without any significant changes in the bond lengths and angles. The ground-state energies of the optimized geometry corresponding to the various spin states are presented in Table S2 of the Supporting Information, which establishes that the septet state is the most stable state, and, in particular, the antiferromagnetic singlet is 0.904 eV less stable than the septet state. All the optimization-related calculations corresponding to different spin states, effect of basis set, and functionals have been performed in the Gaussian 03[12] suite of programs. The geometry optimization has been carried out using B3LYP[13,14] functional in combination with 6-31+G(d, p) basis set for C, H atoms and LANL2DZ + ECP basis for Co and Au atoms. In the optimized structure, Au−Co, C−Co, and C−C bond lengths are 2.43, 1.95, and 1.40 Å, respectively. To investigate the effect of basis set on the optimized structure of the system, we have reoptimized Au (111)−CBC−Au (111) with 6-311+G(d, p) basis set for C, H atoms keeping LANL2DZ + ECP basis fixed for Co and Au. We have found that the change in basis set incorporates an insignificant alteration in the aforementioned bond lengths after the third/fourth decimal point. To check the role of the exchange-correlation functional, we have used another hybrid functional, PBE0,[15] in combination with 6-31+G(d,p) basis set for C and H and LANL2DZ + ECP basis for Co and Au atoms. In this case, the estimated bond lengths are 2.42, 1.95, and 1.40 Å for Au−Co, C−Co, and C−C, respectively. This in turn indicates that both basis set and functional have little impact on the optimized geometry of the system.

To ensure the septet state as the correct ferromagnetic ground state, we have calculated the energy and $\langle S^2 \rangle$ of the antiferromagnetic singlet state by adopting the broken symmetry method as implemented in Gaussian 03.[12] The magnetic coupling constant, J_{AB}, is then determined by Yamaguchi's formula.[16] In this calculation, we have considered CBC attached with one Au (111) surface (3×3 Au atoms) on each side explicitly and evaluated the J_{AB} with the same basis sets and functional that have been employed in the geometry optimization. The computed J_{AB} is found to be $+851$ cm^{-1}, indicating strong ferromagnetic interaction between Co atoms. The robustness of J_{AB} has been meticulously scrutinized by changing the pseudopotential and exchange-correlation functional as well. We found that a change in pseudopotential over Co and Au from LANL2DZ to SDD (Stuttgart−Dresden)[17,18] with B3LYP[13,14] functional gives us $J_{AB} = +992$ cm^{-1}. On the other hand, the J_{AB} value with PBE0 functional and LANL2DZ +ECP basis over Co and Au is only $+504$ cm^{-1}. These two calculations clearly indicate that J_{AB} value is sensitive with respect to the chosen pseudopotential and functional. However, the sign of J_{AB} is positive in all these calculations, which demonstrates that the two Co atoms in Au (111)−CBC−Au (111) are strongly ferromagnetically coupled. In the last two calculations, the basis sets for C and H were kept fixed, that is, 6-31+G(d,p).

The spin-polarized quantum transport properties are evaluated by adopting the Keldysh nonequilibrium Green's function (NEGF) technique in the framework of density functional theory (DFT), and the calculations are implemented in ATK 2.0.4.[19] Within ATK 2.0.4,[19] quantum transport properties are evaluated by using the formalism of Brandbyge et al.,[20] which involves a two-probe configuration with two semi-infinite electrodes and a contact region containing the molecular system connected to a part of either electrode. In the present study, from either side of the Au electrodes, two (3×3) layers of Au atoms (nine Au atoms in each layer) participate in the contact region residing in the *xy* plane, and two semi-infinite electrodes are the part of the bulk Au. The two-probe geometry presented in Figure 1 suggests that the Co atoms are adsorbed on the top of one Au atom in each side of the contact region and CBC is lying in the *yz* plane. All the quantum transport calculations are performed on this configuration.

The quantum transport parameters are extracted with PBE functional[21] and single-ζ + polarization basis function for all the elements. This basis function has been used just to reduce the computational time. For the core electrons, the norm conserving Troullier−Martins pseudopotentials[22] have been used. The two-probe configuration is converged with 150 Ry mesh cutoff energy. The Brillouin zone sampling in the direction of transport has been done using the Monck Horst−Pack grid with 500 and 2500 *k*-points. The currents associated with the majority and minority spins are estimated by the spin-polarized version of the Landauer and Büttiker formula.[23−25] The relevant current equation is given by

$$I_\sigma(V) = \frac{e}{h}\int_{\mu_L}^{\mu_R} T_\sigma(E, V_b)[f_L(E - \mu_L) - f_R(E - \mu_R)]\, dE \qquad (1)$$

where $T_\sigma(E,V_b)$ is the spin-dependent transmission coefficient. $f_{L(R)}(E) = (1)/(1 + \exp\{(E - \mu_{L(R)})/kT\})$ is the Fermi function of the metal electrode with chemical potential $\mu_{L(R)} = E_F \pm eV/2$ and Fermi energy E_F.

(12) Frisch, M. J.; et al. *Gaussian 03*; Gaussian, Inc.: Pittsburgh, PA, 2003.
(13) Becke, A. D. *J. Chem. Phys.* **1993**, *98*, 1372.
(14) Lee, C.; Yang, W.; Parr, R. G. *Phys. Rev. B* **1998**, *37*, 785.
(15) Adamo, C.; Barone, V. *J. Chem. Phys.* **1999**, *110*, 6158.
(16) Yamaguchi, K., Takahara, Y., Fueno, T. V., Smith, H., Eds. *Applied Quantum Chemistry*; Reidel: Dordrecht, 1986; p 155.
(17) Dolg, M.; Stoll, H.; Preuss, H. *Theor. Chim. Acta* **1993**, *85*, 441.
(18) Bergner, A.; Dolg, M.; Kuechle, W.; Stoll, H.; Preuss, H. *Mol. Phys.* **1993**, *80*, 1431.
(19) www.atomistix.com.
(20) Brandbyge, M.; Mozos, J.-L.; Ordejón, P.; Taylor, J.; Stokbro, K. *Phys. Rev. B* **2002**, *65*, 165401.
(21) Perdew, J. P.; Burke, K.; Ernzerhof, M. *Phys. Rev. Lett.* **1996**, *77*, 3865.
(22) Troullier, N.; Martins, J. L. *Phys. Rev. B* **1991**, *43*, 1993.
(23) Datta, S. *Electronic Transport in Mesoscopic Systems*; Oxford University Press: New York, 1995.
(24) Zhu, Z. G.; Su, G.; Zheng, Q. R.; Jin, B. *Phys. Lett. A* **2002**, *300*, 658.
(25) Zhu, Z. G.; Su, G.; Zheng, Q. R.; Jin, B. *Phys. Rev. B* **2004**, *70*, 174403.

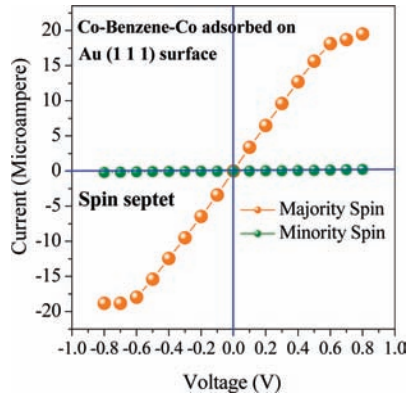

Figure 2. Current−voltage ($I-V$) characteristics of Co−benzene−Co adsorbed on the Au (111) surface in both of the spin channels.

3. Results and Discussion

A variation of the spin-polarized current of CBC system against the applied voltage is depicted in Figure 2. It is evident from this figure that the current for the majority spin is appreciably large as compared to that of the minority spin. Moreover, the current associated with the minority spin does not show any significant variation over the entire range of the bias voltage. This feature certainly establishes the potential of CBC as a molecular spin filter. The equilibrium (zero bias) conductance of the majority spin channel is 30.4618 μS, while the same for the minority spin channel is just 0.148141 μS. The spin filter efficiency in the linear response regime is then calculated from the analysis of transmission characteristics, and it is defined as[10]

$$\mathrm{SFE} = \frac{T_{\uparrow}(E_F) - T_{\downarrow}(E_F)}{T_{\uparrow}(E_F) + T_{\downarrow}(E_F)} \times 100\% \qquad (2)$$

In this equation, $T_{\uparrow}(E_F)$ and $T_{\downarrow}(E_F)$ are the transmission coefficients of the majority and minority spin channels. The calculated spin filter efficiency is found to be 99.03%. As mentioned earlier, the efficiency at the zero bias may not be restored at a finite bias, and to make an unequivocal conclusion on the spin filter efficiency we need to perform the BDSIC calculation. The standard formula of BDSIC is given as follows:

$$\eta = \frac{I_{\text{spin up}} - I_{\text{spin down}}}{I_{\text{spin up}} + I_{\text{spin down}}} \qquad (3)$$

In this equation, $I_{\text{spin up}}$ and $I_{\text{spin down}}$ are the majority and minority spin currents, respectively. A variation of BDSIC against the applied bias voltage is presented in Figure 3. The nature of variation is symmetric about the zero bias, and a BDSIC value as high as 0.991 has been achieved. At relatively higher bias voltage, a slight deviation in BDSIC value is noted with a maximum departure of 0.014. This small deviation is attributed to the apparently unobservable increase of the current in the minority spin channel. It is worth mentioning that a change in k-point sampling from 500 to 2500 does not influence the spin filter action significantly. The spin filter action as manifested in Figures 2 and 3 has been analyzed through the study of spin-polarized transmission spectra of CBC in their spin septet state. A representative finite bias transmission spectrum in both the spin channels of the system is depicted in Figure 4. The figure reveals a strong transmission across the Fermi level, indicating metallic feature of the majority spin, while this feature near the

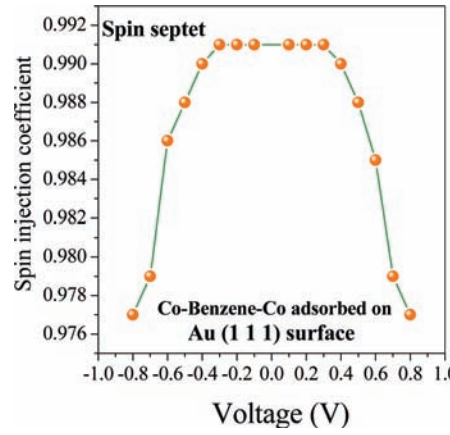

Figure 3. Spin injection coefficient (η) versus bias voltage of the Co−benzene−Co system in the septet state.

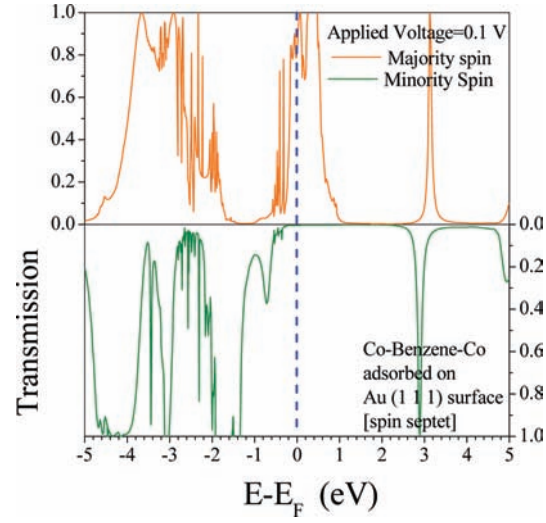

Figure 4. Transmission spectra of Co−benzene−Co adsorbed on the Au (111) surface for both of the spin channels at the bias voltage of 0.1 V.

Fermi level is completely lost in the minority spin channel. To simulate an experimental situation, it is generally accepted that the transmission spectra should show distinctive feature in the two different spin channels over a range of energy close to the Fermi level (E_F). The most prominent aspect of the transmission spectra in a specific spin channel is the transmission peak contributed by the molecular orbital of the central region of two-probe system. In an efficient spin filter, the transmission peaks close to E_F imply resonant tunneling region and contribute directly to the current through the system. In the present study, a wide transmission peak in the vicinity of Fermi level in the majority spin channel quite clearly justifies the emergence of the efficient spin filter action in our anticipated nanodevice (CBC). The transmission spectra of both the spin channels at zero bias are also found to have a feature similar to that in Figure 4 [see the Supporting Information]. We have also evaluated the bias-dependent spin transport parameters for the less stable antiferromagnetic state where both spin channels show identical features with respect to $I-V$ characteristics and transmission spectra, and the corresponding results are presented in the Supporting Information. It is important to mention here that we have considered another configuration, keeping CBC in the xz plane with respect to the electrodes. The details of the orientation are given in the Supporting Information. We found that the SFE in the second configuration, that is, Figure S2 of the Supporting

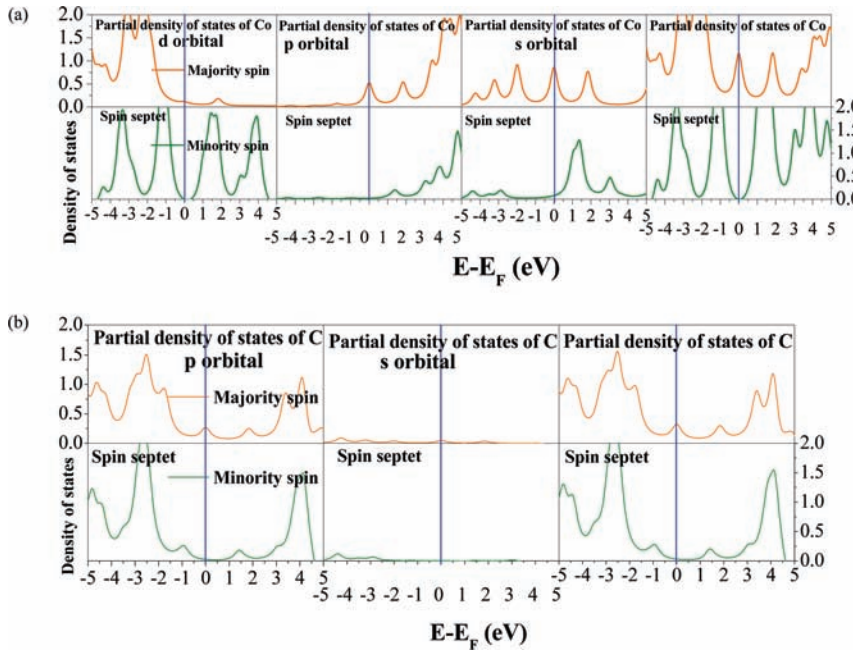

Figure 5. (a) Spin-polarized partial density of states of cobalt including contribution from various orbitals. (b) Spin-polarized partial density of states of carbon including contribution from various orbitals.

Information, is 99.15%, which is marginally the same as that of the first configuration (Figure S1 of the Supporting Information). The quantum transport calculations have also been performed on the optimized geometry of the system obtained from the PBE0 functional, and, in this case too, the CBC system shows strong filter action with SFE = 95.89%.

To make a decisive conclusion on the origin of spin-dependent quantum transport phenomenon in CBC, we have analyzed the spin-polarized total density of states (DOS) and partial density of states (PDOS) of all the elements (C, H, and Co) involved in the system, and the corresponding results for C and Co are presented in Figure 5. The variation of spin-polarized PDOS of Co near the Fermi level gives us a clear revelation of the significant contribution of s and p orbitals in the construction of the singly occupied highest molecular orbital (SOHMO) in the majority spin channel. The spin-polarized PDOS of Co also reflects the missing contribution of 3d orbitals in the SOHMO, which is quite astounding and demands an in-depth analysis of the bonding pattern in CBC. To explain this unusual bonding type, we have performed natural bond orbital (NBO) analysis of CBC in the Gaussian 03 suite of program. We have used the same basis set and functional as that employed in the geometry optimization calculation. The NBO analysis clearly demonstrates significant mixing of the outer-sphere 4s and 4p orbitals of Co, keeping the low-lying unpaired electrons in 3d orbitals inert, and this has happened due to the fact that the nodal structure of d orbital is not favorable for bonding in CBC. At this stage, it is highly instructive to mention here that we have evaluated the spin-polarized PDOS of Co with the explicit inclusion of relativistic interaction and found no significant change in the PDOS corresponding to s, p, and d orbitals of Co in comparison to that of the nonrelativistic data. The spin-polarized PDOS of C shows a contribution from its p orbital at the Fermi level in the majority spin channel, which again is quite unusual because pure benzene has insulating feature in both spin channels. This in turn is a sign of strong coupling between the Co and C atoms of the benzene moiety in the spin septet state, which induces the p orbital of C to partake in the formation of SOHMO. The strong coupling between Co and C is also revealed from the localized magnetic moment (LMM) data over the concerned elements. In case of pure benzene in the septet state, the LMM of the C atoms with which two Co atoms are supposed to be attached in CBC is only 0.06 μ_B, and this value changes to 0.66 μ_B for the same carbon atoms of CBC in the septet state. The calculated value of LMM for each Co atom in CBC is 2.61 μ_B, which is a bit smaller than the expected one. The quenching of LMM of Co and an increment of the same for C indicate a major reorganization of the spin density due to strong coupling between Co and C of the benzene moiety in the septet state. To inspect further, whether the spin filter action of CBC comes purely from the two Co atoms, we have performed a separate electronic structure calculation on Co_2. The determination of the ground state of Co_2 is a challenging task due to the lack of sufficient experimental evidence. Several theoretical attempts have been made to find out the correct ground state of the system. Yanagisawa et al.[26] had applied various levels of density functional approximations along with Hartree−Fock (HF) and Møller−Plesset methods in the study of equilibrium geometry, atomization energy, and interconfigurational energy of the first row transition metal dimer. Shim and co-worker[27] used the HF technique to elucidate the electronic structure of these 3d transition metal dimers. Valiev et al.[28] employed the augmented plane wave approach in the structural analyses of these transition metal dimers. Barden et al.[29] calculated the equilibrium bond distance, vibrational frequency, and dissociation energy of the first row transition metal dimer in the framework of density functional theory. All these theoretical investigations have predicted the spin quintet state as the stable ground state of

(26) Yanagisawa, S.; Tsuneda, T.; Hirao, K. *J. Chem. Phys.* **2000**, *112*, 545.
(27) Shim, I.; Gingerich, K. A. *J. Chem. Phys.* **1983**, *78*, 5693.
(28) Valiev, M.; Bylaska, E. J.; Weare, J. H. *J. Chem. Phys.* **2003**, *119*, 5955.
(29) Barden, C. J.; Rienstra-Kiracofe, J. C.; Schaefer, H. F., III. *J. Chem. Phys.* **2000**, *113*, 690.

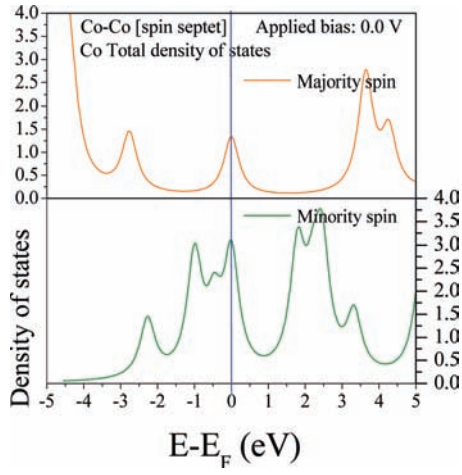

Figure 6. Density of states of bare Co_2 system (septet state).

Co_2, which has further been justified by the work of Gutsev et al.[30] In the present study, we have found that the septet state of Co_2 dimer is more stable (0.54 eV) than its quintet state. In the earlier work of Yanagisawa et al., "Wachter + f"[31−33] basis has been used with wide range of exchange-correlation functionals, and they found that the bond distance between two Co atoms in the $^5\Delta_g$ state is 1.946 Å, while in our calculation we have obtained a Co−Co bond length of 1.96 Å for the same state with LANL2DZ/B3LYP[13,14] level of theory. The bond length of Co_2 in the $^7\Sigma_g^+$ state of our calculation is 2.11 Å. Gutsev et al. have considered the $^7\Sigma_g^+$ state, but they did not use hybrid B3LYP[13,14] functional in their calculation. As a consequence, due to the lack of B3LYP[13,14] results on the $^7\Sigma_g^+$ state of Co_2 in all these earlier calculations, it is difficult to make any final conclusion on the stable ground state of Co_2. Because the true ground state of Co_2 is still unknown at the experimental level, we have performed the DOS calculation of Co_2 at both spin states, quintet and septet states. We have presented the DOS of the septet state in Figure 6, and the DOS of the quintet state is shown in Figure S9 of the Supporting Information. A finite DOS across the Fermi level in the majority and minority spin channels is revealed for both the septet and the quintet spin states. This indicates that the nature of DOS of a bare Co_2 molecule in the spin septet and quintet states is completely different from that of the PDOS of the Co atoms in CBC. Thus, the spin-polarized PDOS of Co and C along with other relevant calculations suggest that the spin filter action in CBC is not originated from the low energy 3d unpaired electrons of Co like in the other transition metal−organic framework, but rather a mixing of 4s and 4p orbitals of Co through the promotion of an electron from 4s → 4p is responsible for the strong bonding between Co and C of the benzene moiety, and this 4sp-hybridized orbital of Co has made an important contribution to the formation of SOHMO, which finally is responsible for the coherent spin transport in CBC.

The SOHMOs of CBC with two layers of Au in both the spin channels are extracted by solving the eigenstates of the well-known molecular projected self-consistent Hamiltonian (MPSH). The finite MPSH matrix is expressed as[34]

$$\begin{bmatrix} H_L + \Sigma_L & V_L & 0 \\ V_L^\dagger & H_C & V_R \\ 0 & V_R^\dagger & H_R + \Sigma_R \end{bmatrix} \quad (4)$$

where H_L, H_R, and H_C are Hamiltonian matrices in the left electrode (L) and right electrode (R) and contact region (C), respectively. Likewise, V_L and V_R are the interaction potential between the L−C and L−R regions, respectively. Σ_L and Σ_R represent self-energies of the left and right electrode, respectively. It is worth noting that the Landauer approach does not include the explicit interaction between the bridge and tunneling electrons, and transmission is not directly dependent upon occupation number in a particular molecular orbital. However, the spin states have a strong influence on the shape of the molecular orbital and have a profound impact on the transmission spectra of the system. In our case, the MPSH states corresponding to the SOHMO of CBC in both the spin channels at a representative finite bias voltage of 0.1 V are shown in Figure 7. The figure demonstrates that the SOHMO isosurface in the majority and minority spin channel possess completely different characteristics. In the majority spin channel, charge density is delocalized over the molecule and Au electrodes. The contribution of the p orbital of C and sp-hybridized orbital of Co in the SOHMO of the majority spin channel can also be qualitatively visualized from the Figure 7. On the other hand, the charge density in the SOHMO of the minority spin channel has the dominant amplitude centered over the left-hand Au electrode leaving practically zero density over the benzene moiety and the Co atom attached with the right-hand electrode. The delocalized charge density in the SOHMO of the majority spin channel provides a distinct metal-like conduction path, while the strong localization of charge density in the SOHMO of the minority spin channel can give us an insignificant current contribution through tunneling, which at the end is responsible for the high spin injection coefficient of CBC in the septet state.

4. Conclusion

In conclusion, the present investigation reports exceptionally high spin injection coefficient of the nanodevice comprised of the ferromagnetically coupled Co−benzene−Co system adsorbed on Au (111) surface. At finite bias, the spin filter efficiency index of CBC (0.991) is unprecedented. The genesis of this simulated spin filter action has been critically examined by a wide range of theoretical analyses, and to our utter astonishment we found that the low-lying unpaired 3d electrons of Co do not make any contribution to the spin filter action in CBC like other transition metal containing multidecker wires,

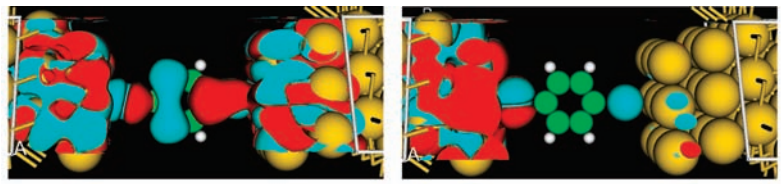

(SOHMO of majority spin; Applied bias: 0.1V) (SOHMO of minority spin; Applied bias: 0.1V)

Figure 7. Spin-polarized molecular projected self-consistent Hamiltonian (MPSH) states of Co−benzene−Co adsorbed on Au (111) surface at the bias voltage of 0.1 V.

but rather the spin filter action in this material comes from the mixing of the outer-sphere 4s and 4p orbitals of Co and a partial contribution of the 2p orbitals of C. Thus, the origin of spin filter action in CBC is quite unique, and to the best of our knowledge this is the first one of its own kind. Finally, we strongly believe that the proposed spintronic nanodevice has the potential to initiate a variety of new exciting applications and motivate experimentalists to design such small organic spin filters in the future.

Acknowledgment. We convey our special thanks to Atomistix Inc. for allowing us to use ATK 2.0.4 for quantum transport calculations. The financial support from DST, Govt. of India (Under FIST Program), to purchase the Gaussian 03 program is gratefully acknowledged. S.C. acknowledges the centre for nanoscience and nanotechnology, University of Calcutta, for research funding.

Supporting Information Available: Tabular representation of spin injection coefficient, $I-V$ characteristics of spin singlet state, transmission spectra of spin septet and spin singlet configuration at zero bias voltage, energy dispersion curve of benzene in spin septet state as well as Co−benzene−Co in spin septet state, density of states of the Co−benzene−Co system (septet state) including partial density of states of C and Co, density of states of bare Co−Co system (septet state), and MPSH states at 0 V corresponding to spin septet and singlet state. This material is available free of charge via the Internet at http://pubs.acs.org.

JA106705M

(30) Gutsev, G. L.; Khanna, S. N.; Jena, P. *Chem. Phys. Lett.* **2001**, *345*, 481.
(31) Wachters, A. J. H. *J. Chem. Phys.* **1970**, *52*, 1033.
(32) Wachters, A. J. H. IBM Technical Report No. RJ584, 1969.
(33) Bauschlicher, C. W., Jr.; Langhoff, S. R.; Barnes, L. A. *J. Chem. Phys.* **1989**, *91*, 2399.
(34) Sen, S.; Chakrabarti, S. *J. Phys. Chem. C* **2008**, *112*, 1685–1693.